



Glycoluril–tetrathiafulvalene molecular clips: on the influence of electronic and spatial properties for binding neutral accepting guests

Yoann Cotelle, Marie Hardouin-Lerouge, Stéphanie Legoupy, Olivier Alévêque, Eric Levillain* and Piétrick Hudhomme*

Full Research Paper

Open Access

Address:
Université d'Angers, Laboratoire MOLTECH-Anjou, CNRS UMR 6200,
2 Boulevard Lavoisier, F-49045 Angers, France

Email:
Eric Levillain* - eric.levillain@univ-angers.fr;
Piétrick Hudhomme* - pietrick.hudhomme@univ-angers.fr

* Corresponding author

Keywords:
donor–acceptor interactions; glycoluril; molecular clips;
supramolecular chemistry; tetrathiafulvalene

Beilstein J. Org. Chem. **2015**, *11*, 1023–1036.
doi:10.3762/bjoc.11.115

Received: 13 March 2015
Accepted: 28 May 2015
Published: 17 June 2015

This article is part of the Thematic Series "Tetrathiafulvalene chemistry".

Guest Editor: P. J. Skabara

© 2015 Cotelle et al; licensee Beilstein-Institut.
License and terms: see end of document.

Abstract

Glycoluril-based molecular clips incorporating tetrathiafulvalene (TTF) sidewalls have been synthesized through different strategies with the aim of investigating the effect of electrochemical and spatial properties for binding neutral accepting guests. We have in particular focused our study on the spacer extension in order to tune the intramolecular TTF...TTF distance within the clip and, consequently, the redox behavior of the receptor. Carried out at different concentrations in solution, electrochemical and spectro-electrochemical experiments provide evidence of mixed-valence and/or π -dimer intermolecular interactions between TTF units from two closed clips. The stepwise oxidation of each molecular clip involves an electrochemical mechanism with three one-electron processes and two charge-coupled chemical reactions, a scheme which is supported by electrochemical simulations. The fine-tunable π -donating ability of the TTF units and the cavity size allow to control binding interaction towards a strong electron acceptor such as tetrafluorotetracyanoquinodimethane (F₄-TCNQ) or a weaker electron acceptor such as 1,3-dinitrobenzene (*m*-DNB).

Introduction

Thanks to its remarkable redox properties and strong π -donating character demonstrated with the pioneering work of F. Wudl in the early 1970s [1], tetrathiafulvalene (TTF) has become one of the most popular electroactive frameworks used in materials

science [2-5]. In addition to the well-known access to molecular conductors [6,7] and TTF-acceptor assemblies [8,9], new concepts have been explored in the field of supramolecular chemistry using the TTF unit as a powerful electroactive

building block [10]. Exploiting its peculiar electronic (two successive reversible oxidation steps giving rise to three stable redox states) characteristics, more and more sophisticated TTF-based supramolecular systems have been designed, being able to operate as machines, chemical sensors, redox-switchable ligands, molecular shuttles, molecular switches and logic gates [11]. Considering that molecular receptors prone to specifically recognize neutral molecules through donor–acceptor interactions are of particular interest [12], the unique π -donating ability and the planar geometry of the TTF building-block are suited to the construction of such receptors. Nevertheless, the incorporation of TTF as a π -donating element in molecular clips or tweezers for recognition of neutral electron acceptor guests is still relatively unexplored [13].

Molecular clips and tweezers can be defined as receptors presenting an open cavity composed of two interaction sites which are separated by a spacer [13–15]. Ideally, these systems are designed with the aim of sandwiching a molecular guest with a high degree of selectivity and control of the interactions between the guest and the sidewalls. While the nature and the flexibility of the spacer between the two sidewalls play a critical role in the recognition process, we were interested in rigidifying the molecular clips in order to favor the “lock and key” model [15]. This rigid structure offers the possibility to orient the interaction sites in a defined manner allowing an increase of the binding strength with the guest. In the last two decades, glycoluril-based molecular clips have shown that they were capable of acting as excellent receptors by exploiting the distance between the two aromatic sidewalls which is usually close to 7 Å. Since then, a large number of host systems based on this

principle have been synthesized in order to use them for recognition of aromatic guest molecules through π – π interactions [16,17].

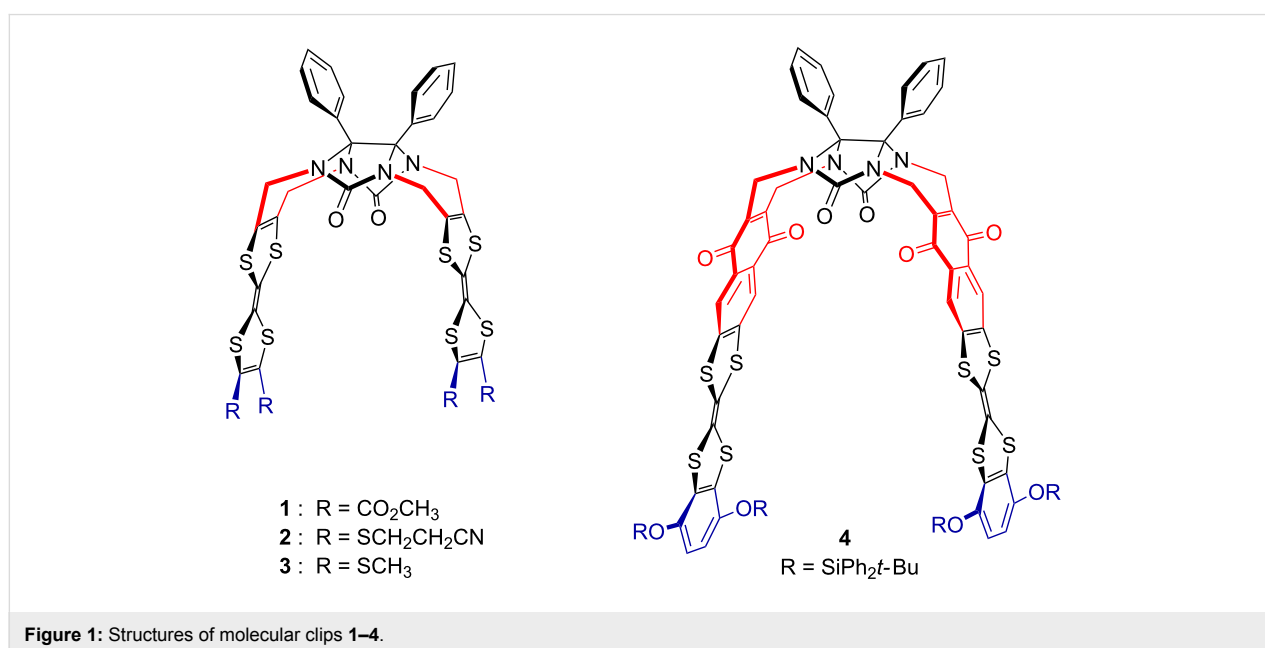
We recently described various glycoluril-based molecular clips **1–4** [18,19] (Figure 1) for which the structure varies by: i) the nature of connection between the glycoluril spacer and the TTF sidewalls, ii) the nature of the peripheral substituents on both TTF pincers. In this full research paper we propose to study how these structural parameters influence the electron donating ability of TTF pincers and the size of the cavity and how the control over the inter-TTFs distance within the molecular clip impacts the ability for sandwiching neutral acceptor guests. Those studies are supported by electrochemical analyses (including simulation), time-resolved spectroelectrochemical experiments and UV–visible titrations.

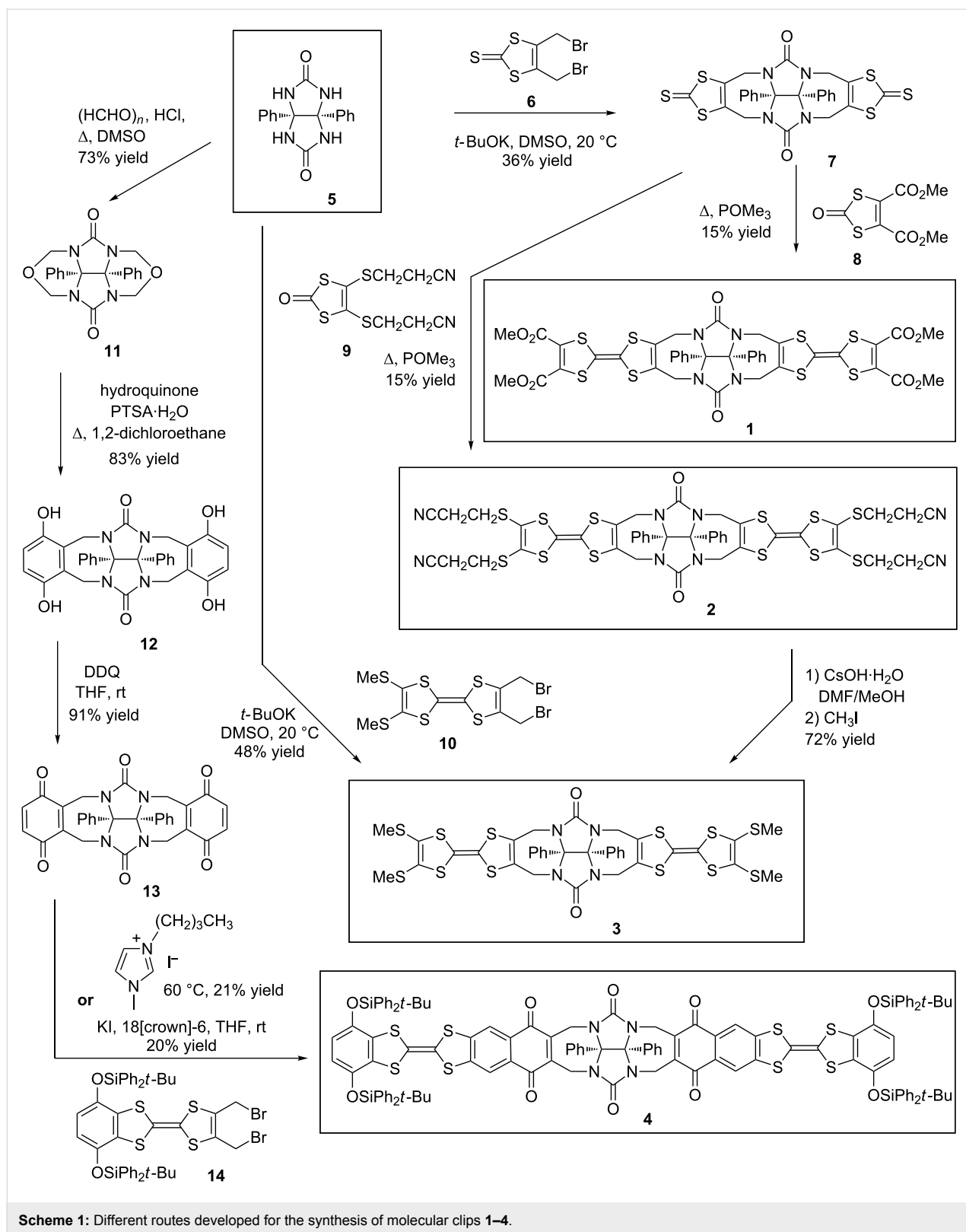
Results and Discussion

Synthesis

We have designed molecular clips **1–4** through three different synthetic strategies starting from diphenylglycoluril **5** (Scheme 1). The key building-block **5** is available in multigram scale by reaction of benzil with urea [20]. The first approach leading to molecular clips **1** and **2** is based on a straightforward double nucleophilic substitution leading to a seven-membered ring using 4,5-bis(bromomethyl)-2-thioxo-1,3-dithiole (**6**) [21].

In order to determine the optimized experimental procedure to carry out the urea N-alkylation of compound **5**, we took advantage from literature of previous works realized on glycoluril for such reaction using a 2,3-bis(halogenomethyl)aryl derivative.





Reported procedures were using KOH [22,23], *t*-BuOK [24–26] or NaH [27] as the base with DMSO as an aprotic polar solvent. Different experimental conditions were tested for the reaction

between diphenylglycoluril **5** and 4,5-bis(bromomethyl)-2-thioxo-1,3-dithiole (**6**) as the electrophilic reagent (Scheme 2) by varying parameters such as the nature of the base, the reac-



Scheme 2: Reaction between diphenylglycoluril with 4,5-bis(bromomethyl)-2-thioxo-1,3-dithiole.

tion time and the temperature (Table 1). Optimal conditions were using four equivalents of *t*-BuOK in anhydrous DMSO by keeping the temperature at 20 °C with a cryostat apparatus for 3 h. Compound 7 was isolated in 36% yield after purification by silica gel chromatography. We should note that an increase of temperature resulted in the degradation of starting material 6.

Table 1: Optimized experimental conditions for the synthesis of compound 7.

Base	Temperature (T)	Reaction time (t)	Yield [%]
KOH	rt	24 h	6
NaH	rt	24 h	5
KOH	rt	4 h	12
<i>t</i> -BuOK	rt	4 h	19
<i>t</i> -BuOK	Controlled 30 °C	4 h	12
<i>t</i> -BuOK	Controlled 20 °C	3 h	36

This first strategy to reach clips 1 and 2 was considering the trimethylphosphite-mediated cross-coupling reaction involving 2-oxo-1,3-dithiole moiety 8 [28] as an efficient route to prepare dissymmetrical TTF derivatives [29]. The polarity of compounds which were formed was sufficiently different to allow an efficient purification by silica gel chromatography affording molecular clip 1 in 15% yield. This route was successfully applied using compound 9 [30] and clip 2 was also isolated in 15% yield. Target clip 3 was finally obtained in 72% yield by deprotection of precursor 2 using CsOH·H₂O in DMF/MeOH mixture [31], followed by the tetraalkylation of tetrathiolate with iodomethane. Considering that this multi-step synthesis was affording molecular clip 3 in an overall 4% yield starting from diphenylglycoluril 5, we took advantage of the accessibility of 2,3-bis(bromomethyl)TTF 10 [32] bearing methylsulfanyl groups to investigate a more straightforward strategy. Alternatively, the above methodology described for the preparation of compound 7 was efficiently applied to reach molecular clip 2 in 48% yield using similar experimental conditions.

Whereas the synthesis of molecular clips 1, 2 and 3 uses the nucleophilic substitution onto diphenylglycoluril 5 as a key-

step, the introduction of the naphthoquinone spacer in clip 4 required the previous transformation of compound 5 into a glycoluril-based framework possessing quinone moieties for developing a Diels–Alder cycloaddition strategy. Thus compound 12 [33] was prepared in 73% yield by treatment with an excess of hydroquinone in 1,2-dichloroethane using a Friedel–Crafts alkylation as an electrophilic aromatic substitution onto compound 11 [34]. The hydroquinone moieties were subjected to a dehydrogenation reaction using DDQ in THF to reach desired glycolurildiquinone 13 [35] in 91% yield. The Diels–Alder cycloaddition was carried out by treatment of bis-dienophile 13 with TTF derivative 14 [36], able to give rise in situ to the transient diene by reductive elimination using naked iodide [37–39] or the iodo-ionic liquid 1-butyl-3-methylimidazolium iodide [40]. After purification by column chromatography on silica gel, we noted that complete aromatization has occurred concomitantly and molecular clip 4 was isolated in around 20% yield.

Whereas all attempts at growing crystals of molecular clips 1 and 4 of sufficient quality for X-ray analysis have been unsuccessful so far, suitable single crystals were obtained by slow diffusion from a solution of clips 2 and 3 in a CH₂Cl₂/hexane mixture. Considering the central double bond of each TTF moiety, the intramolecular wall-to-wall distance was determined to be equal to 8.25 Å and 7.41 Å for clip 2 and 3, respectively (Figure 2) [18]. Then the corresponding wall-to-wall distance between the two TTF units was determined by theoretical calculations using the semi-empirical AM1 method in the case of 4 [19]. This distance was estimated to be equal to 9.7 Å indicating that this enlargement around 2 Å was the result mainly of the spatial contribution of the additional naphthoquinone spacer in molecular clip 4.

Electrochemical properties

The electrochemical behaviour of molecular clips 1–4 were determined using cyclic voltammetry experiments (Table 2).

These studies displayed a different electrochemical behavior for clips 1, 2 and 3 in comparison to clip 4. In the latter case, the cyclic voltammogram (CV) showed two oxidation waves at

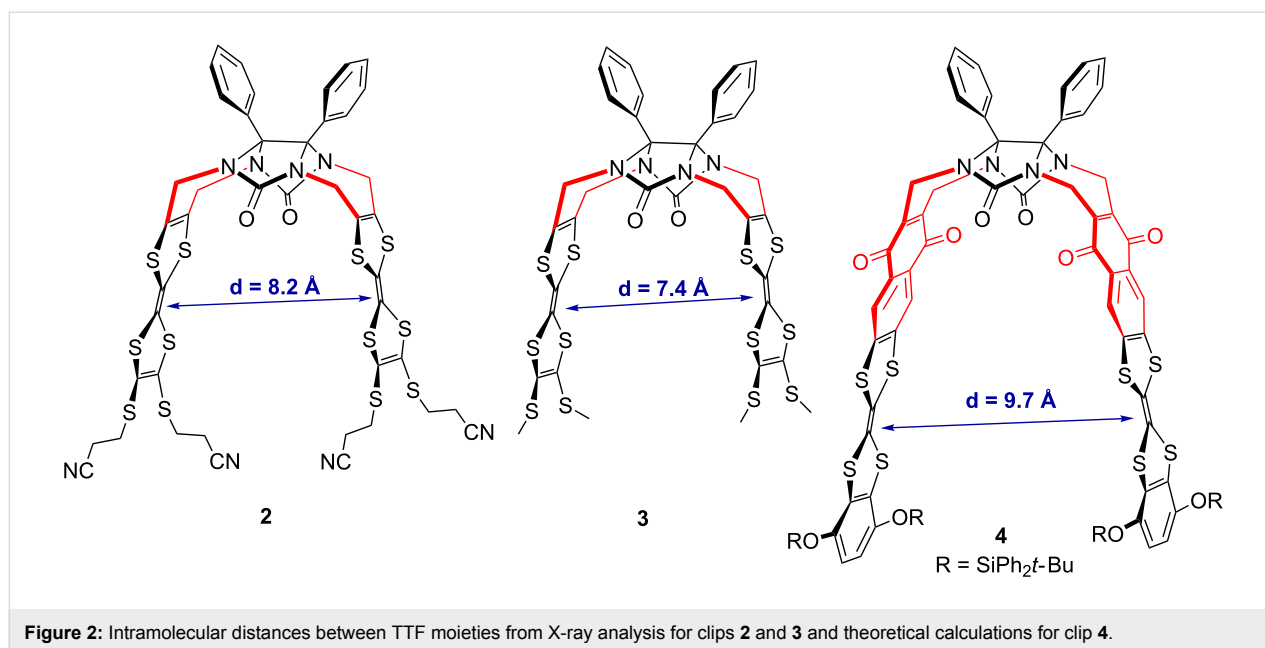


Table 2: Apparent redox potentials of molecular clips **1**, **2**, **3** and **4** reported vs Fc^+/Fc in 0.1 M $\text{TBAPF}_6/\text{CH}_2\text{Cl}_2/\text{CH}_3\text{CN}$ 3:1 on glassy carbon electrode at $100 \text{ mV}\cdot\text{s}^{-1}$. Absolute errors on potentials were found to be around $\pm 10 \text{ mV}$.

Clip	$E_{\text{app}}^0_{\text{red1}}$	$E_{\text{app}}^0_{\text{ox1}}$	$E_{\text{app}}^0_{\text{ox1}'}$	$E_{\text{app}}^0_{\text{ox2}}$
1	–	+0.06	+0.21	+0.51
2	–	+0.03	+0.14	+0.45
3	–	–0.05	+0.06	+0.36
4	–1.05	+0.28		+0.65

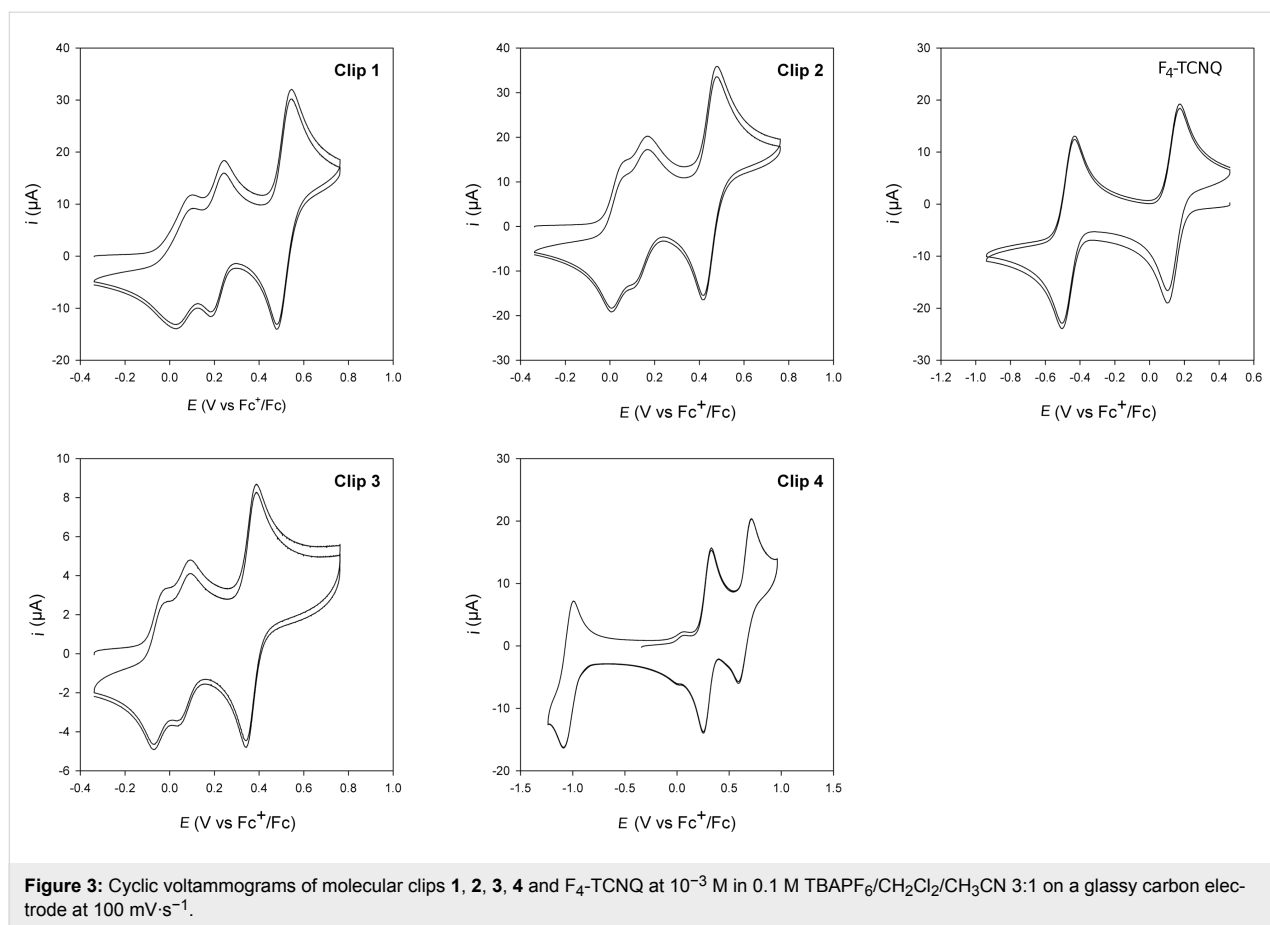
$E_{\text{app}}^0_{\text{ox1}} = +0.28 \text{ V}$ and $E_{\text{app}}^0_{\text{ox2}} = +0.65 \text{ V}$ vs Fc^+/Fc corresponding to the successive generation of cation radical then dication species simultaneously on each TTF framework (Figure 3). This unique first two-electron oxidation step indicates that the two TTF units are electrochemically equivalent, thus excluding the presence of intra- or intermolecular electronic interactions between them. It should be noted that the electroactive naphthoquinone acceptor group incorporated in the spacer unit is characterized by a reduction wave ($E_{\text{app}}^0_{\text{red1}}$) at -1.05 V vs Fc^+/Fc . On the contrary, the CV of clips **1–3** shows a significant splitting of the first oxidation wave ($E_{\text{app}}^0_{\text{ox1}}$ and $E_{\text{app}}^0_{\text{ox1}'}$), suggesting the presence of intermolecular (between two clips) or intramolecular (within a clip) interactions between two TTF units (i.e., mixed valence and/or π -dimer) [41]. Eventually, the reversible two-electron process (i.e., 1 e^- on each TTF^+ unit) for the second oxidation step ($E_{\text{app}}^0_{\text{ox2}}$) leading to fully oxidized TTF units is in accordance with independent TTF^{2+} states subject to repulsive electrostatic interactions. Such splitting phenomenon of the first oxidation wave has been previously reported by Azov et al. for TTF-containing molecular

tweezers based on a 1,2,4,5-tetramethylbenzene scaffold [42,43].

At this stage, one should keep in mind that the distance between two TTF sidewalls within clips **2** and **3** is quite important (8.2 \AA and 7.4 \AA , respectively). Such a distance, even though determined in the solid state, does not seem compatible to allow an intramolecular interaction to occur between two TTF units during the first oxidation step. In order to address this issue and to explore possible intermolecular (between two clips) interactions, concentration dependence electrochemical experiments were performed. Cyclic voltammograms were recorded using molecular clip **2** at different concentrations (10^{-3} M , 10^{-4} M and $5 \times 10^{-5} \text{ M}$) (Figure 4).

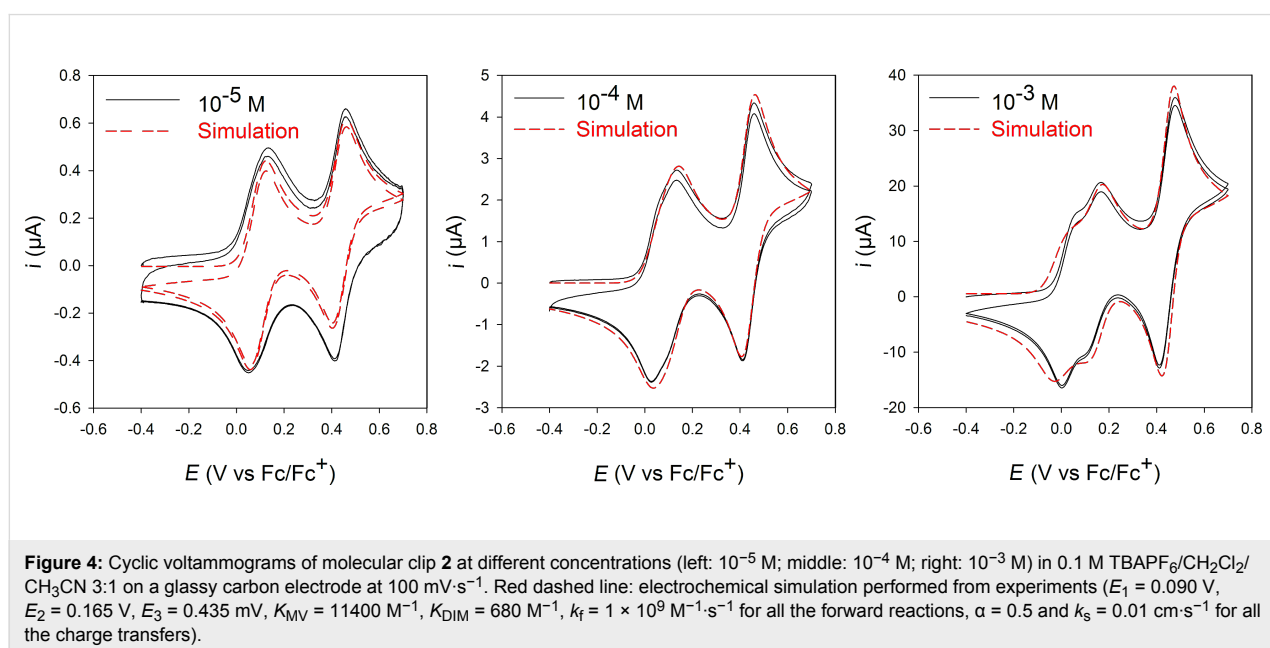
Importantly, whereas the splitting of the first oxidation wave was perfectly observed at high concentration (10^{-3} M), we noted that the phenomenon was significantly decreased at lower concentration. First, the absence of a splitting or broadening of the first oxidation process at low concentration informed us that the two TTF units are equivalent, thus excluding intramolecular interactions. Secondly, the concentration dependence and the splitting at higher concentrations provided evidence for the existence of intermolecular interactions and the formation of mixed-valence and radical cation dimer states. These results clearly demonstrated the presence of an intermolecular mixed-valence phenomenon.

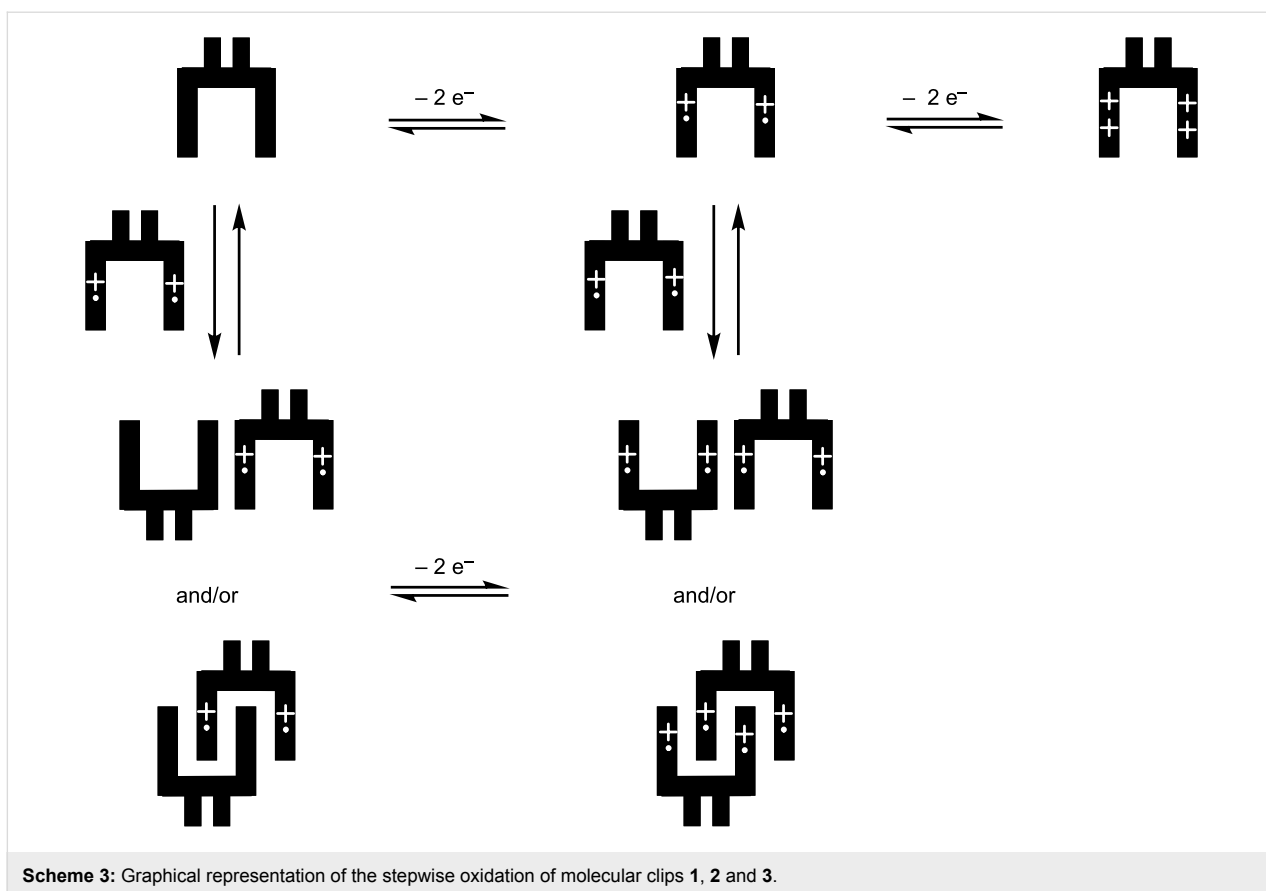
According to these first results, the following model could be proposed in agreement with the successive oxidation steps in the CV of molecular clips **1**, **2** and **3** (Scheme 3). Because the



two TTF units are equivalent, the first oxidation step of the clip involves a one-electron process on each TTF unit, leading to the clip bearing two radical cations. The concentration dependence

shown on CVs suggested that this clip with two radical cations stack with and/or without self-assembly affording mixed-valence or π -dimer interactions. At higher potential, the tetra-

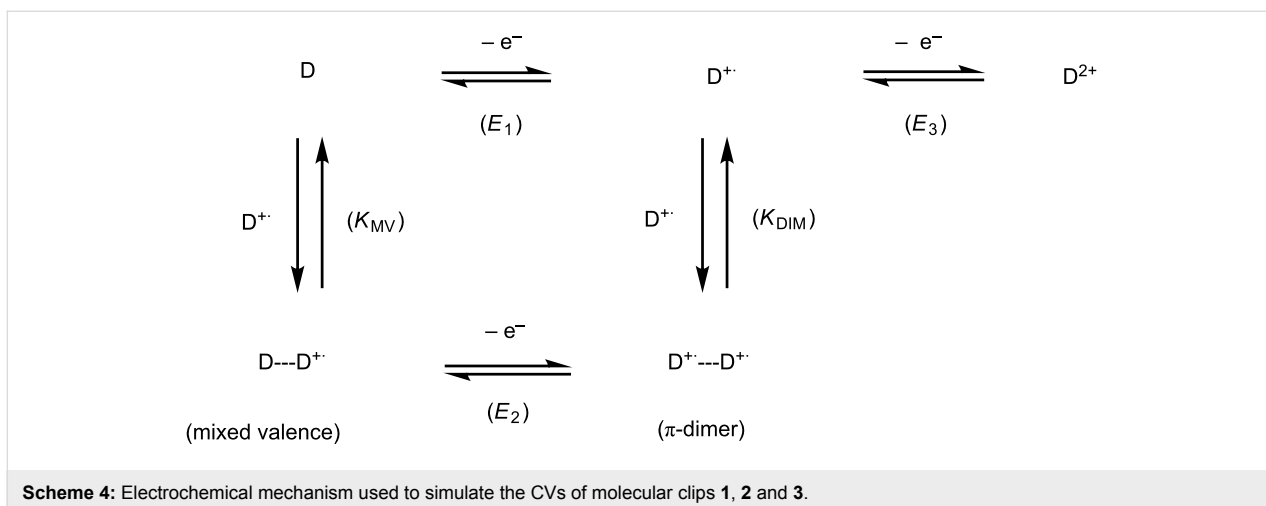




cation is provided by another one-electron process on each TTF unit leading to a clip bearing two dications.

The graphical representation can be simulated by an electrochemical simulation program (DigiElch 7) involving an electrochemical mechanism (Scheme 4) composed by three one-electron processes and two charge-coupled chemical reactions (i.e., formation of mixed-valence and dimerization via a square

scheme). Due to the equivalence of the two TTF units, it is important to note that the input value of the concentration of **D** in Scheme 4 (**D** represents one TTF unit of the clip) must be twice that of the experimental concentration of a molecular clip. The good agreement between experimental data and modelled CVs over the whole range of concentration supports the graphical representation of the stepwise oxidation of molecular clips **1**, **2** and **3** (Scheme 3).



Optical and spectroelectrochemical properties

The optical properties of oxidized states of molecular clip **1** were monitored by UV–vis–NIR spectroscopy, by successive aliquot addition of NOSbF_6 (5×10^{-3} M in CH_3CN) used as oxidizing reagent in a solution of clip **1** (10^{-4} M in CH_2Cl_2) in a quartz cell (0.2 cm) (Figure 5). Clip **1** bearing methoxycarbonyl groups at the periphery of the TTF framework was chosen because, to our knowledge, the optical characteristics of such a TTF derivative have not been yet reported. The redox potential (+ 0.87 V vs Fc^+/Fc) of the NOSbF_6 reagent is in agreement to allow the oxidation of TTF units. Chemical oxidation led to the rapid disappearance of the band at 320 nm attributed to the neutral TTF derivative and to the concomitant development of new bands characteristic for the cation radical and/or the π -dimer (440, 595 nm), bands which are characteristic for substituted TTF derivatives. After addition of nearly two equivalents of oxidizing reagent, we noted the appearance of the absorption band characteristic of the formation of the TTF dication (340 nm). As soon as we started to add aliquots of NOSbF_6 oxidant onto molecular clip **1**, we could observe in the NIR region an absorption band centered at approximately 815 nm and a broad and weak band between 1300–2000 nm.

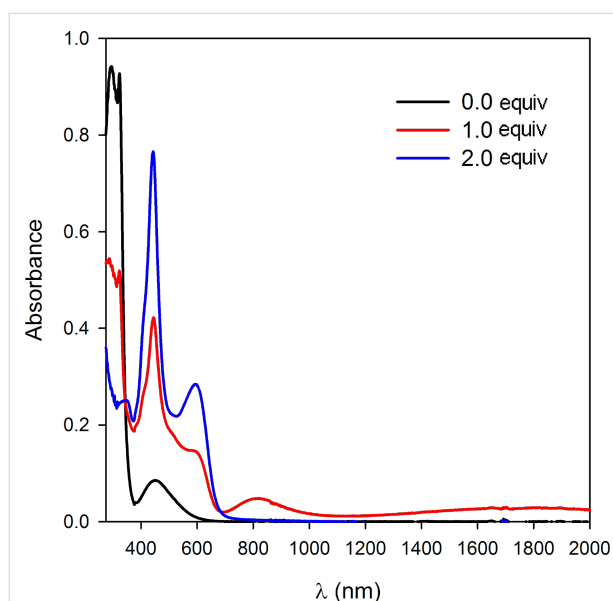


Figure 5: Chemical oxidation of molecular clip **1** (10^{-4} M, CH_2Cl_2) using aliquots of NOSbF_6 oxidizing reagent (5×10^{-3} M, CH_3CN).

Known to be a powerful tool for analyzing the formation of π -dimers (DIM) and mixed-valence (MV) systems, time resolved spectroelectrochemical experiments [44–46] were performed on molecular clip **1** in order to probe the first oxidation step at two different concentrations between 350 and 1700 nm in 0.1 M $\text{TBAPF}_6/\text{CH}_2\text{Cl}_2/\text{CH}_3\text{CN}$ (3:1). At

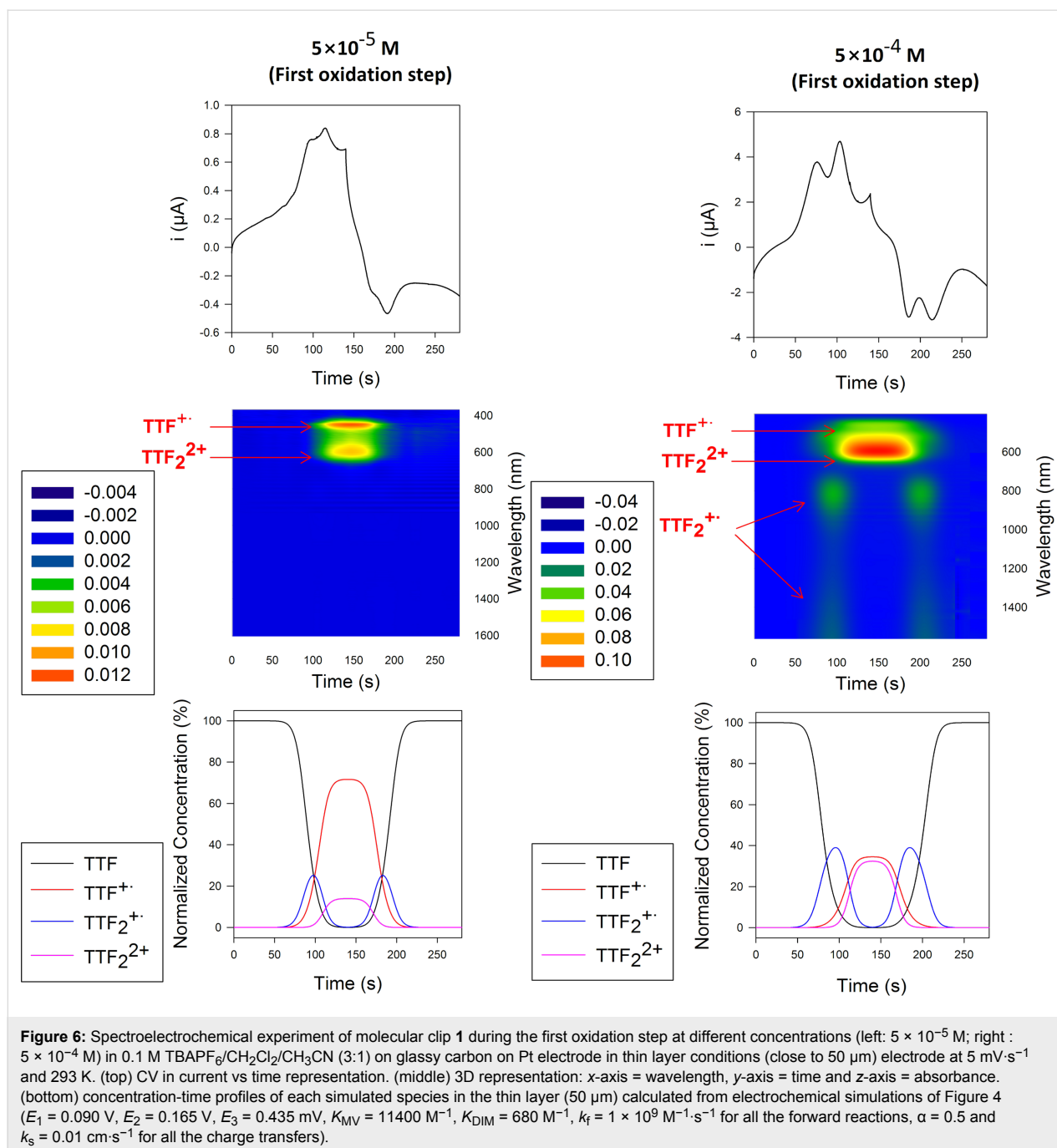
5×10^{-5} M, only two absorption bands (i.e., 450 and 600 nm) were observed (Figure 6). Confirming a concentration dependence, the absorbance profile at 5×10^{-4} M was different from the one obtained at 5×10^{-5} M. Two additional absorption bands simultaneously emerged at the beginning of the oxidation process and the end of the reduction process: one at 825 nm and a broad band in near infrared range beyond 1300 nm (Figure 6).

In agreement with the simulated concentration–time profiles in thin layer conditions (Figure 6 – bottom), the appearance of the absorption bands centered around 825 and beyond 1300 nm were attributed to the formation of $[(\text{TTF})_2]^+$ mixed-valence dimer [47,48] and the absorption bands centered around 600 nm to the $(\text{TTF}^+)_2$ π -dimer [49]. The band close to 825 nm could be assigned to cation radicals stack with self-assembly affording mixed-valence. Nevertheless, at this stage, it would be premature to conclude with certainty. The origin of this band is currently under investigation and requires complementary studies to carry out on different substituted molecular clips.

By analogy with unsubstituted TTF derivative, these three bands reasonably support the presence of mixed-valence and cation radical dimers during the oxidation process. Whereas the phenomenon of dimer formation of the TTF cation radical is commonly observed in the solid state, it was also described in solution at low temperature in a concentrated TTF solution [50], or at room temperature in a dilute solution. In the latter case, the characterization of $[(\text{TTF})_2]^{+}$ mixed-valence dimer and/or $(\text{TTF}^+)_2$ dimer species concerned systems for which the dimer stabilization is resulting from the close proximity of the two TTF units. That is the case for conjugated bisTTF systems [51], bisTTF-substituted calix[4]arenes [52], or supramolecular architectures such as [3]catenane [53], cucubit[8]uril [54] or self-assembled cages [55] which facilitate the formation of TTF dimers.

Studying the glycoluril-based molecular clip **15** presenting also TTF sidewalls [56,57], Chiu et al. have observed the mixed-valence and radical cation dimer states at high concentration (10^{-3} M) and at room temperature [58]. Indeed, the CV of molecular clip **15** exhibited four consecutive oxidation waves, which were interpreted by a succession of oxidation processes of the TTF sidewalls (Figure 7). These dimer interactions were predicted to exist at room temperature by theoretical investigation realized on this system [59].

By comparison with these results observed for molecular clip **15** [58], it is clear that clips **1–3** exhibit $[(\text{TTF})_2]^{+}$ mixed-valence dimer and/or $(\text{TTF}^+)_2$ dimer species but their self-association organization could not be yet demonstrated. The



presence of more or less sterically bulky groups at the periphery of the TTF moieties does not provide an advantage for the self-assembly of dimers. Moreover, this dimerization phenomenon which is driven by the inclusion of one sidewall into the cavity of the opposing clip is not observed in the solid state for clips **2** and **3** (Figure 8). This typical packing arrangement was previously observed in many cases of glycoluril-based molecular clips containing two aromatic sidewalls [26,60–63]. On the contrary, considering the unit cell for single crystals of clip **2**, X-ray analysis showed that two neighboring molecules of clip **2**

appeared in a head-to-tail arrangement and short TTF...TTF intermolecular distances (3.51 Å) were determined between two clips in the solid state.

Binding properties

In order to establish the influence of electronic and spatial properties of the clips towards binding ability of neutral electrodeficient guest molecules, we have chosen compounds **3** and **4** for this study. Molecular clip **3** presents better π -donating ability according to CV study and a smaller interplanar TTF distance

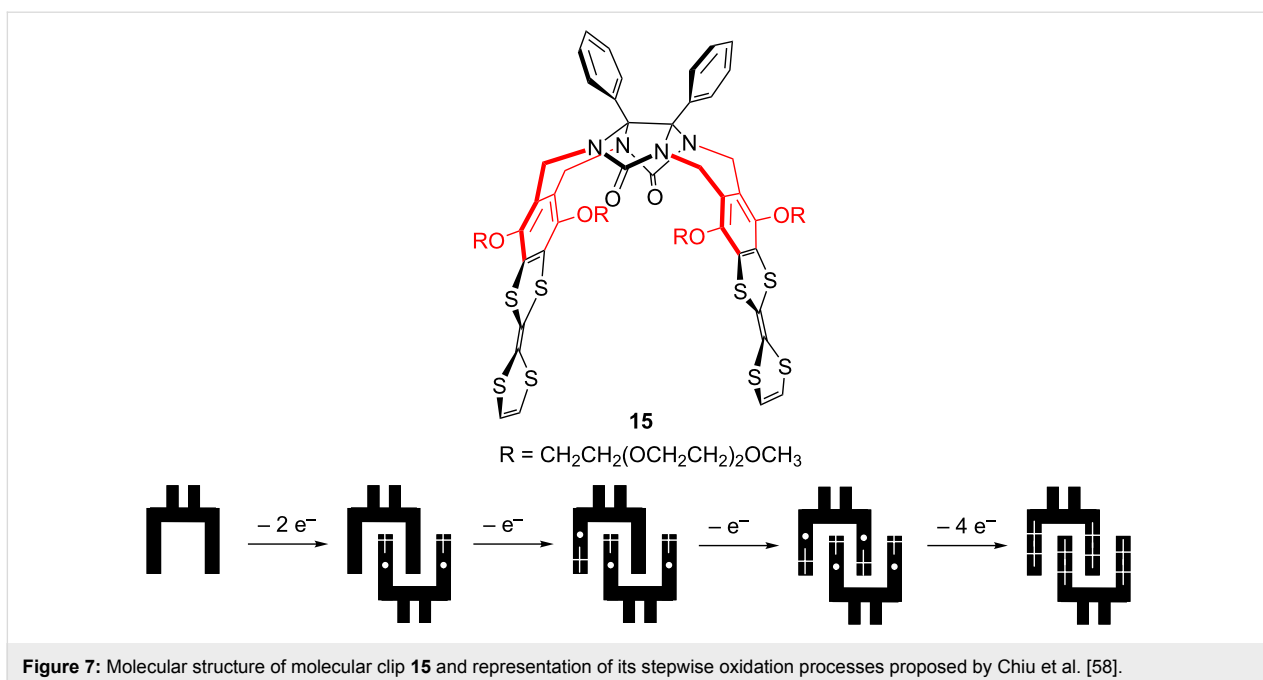


Figure 7: Molecular structure of molecular clip **15** and representation of its stepwise oxidation processes proposed by Chiu et al. [58].

(7.41 Å compared to calculated 9.2 Å for clip **4**). Binding properties were studied using 1,3-dinitrobenzene (*m*-DNB) as a weak and small aromatic electron acceptor molecule. It should be noted that Nolte et al. have successfully observed the com-

plexation of *m*-DNB using a glycoluril-based receptor bearing 2,7-dimethoxynaphthalene walls ($K_a = (115 \pm 10) \text{ M}^{-1}$) [64]. In the latter case, it was proposed that binding was occurring through an induced-fit mechanism with a recognition process on

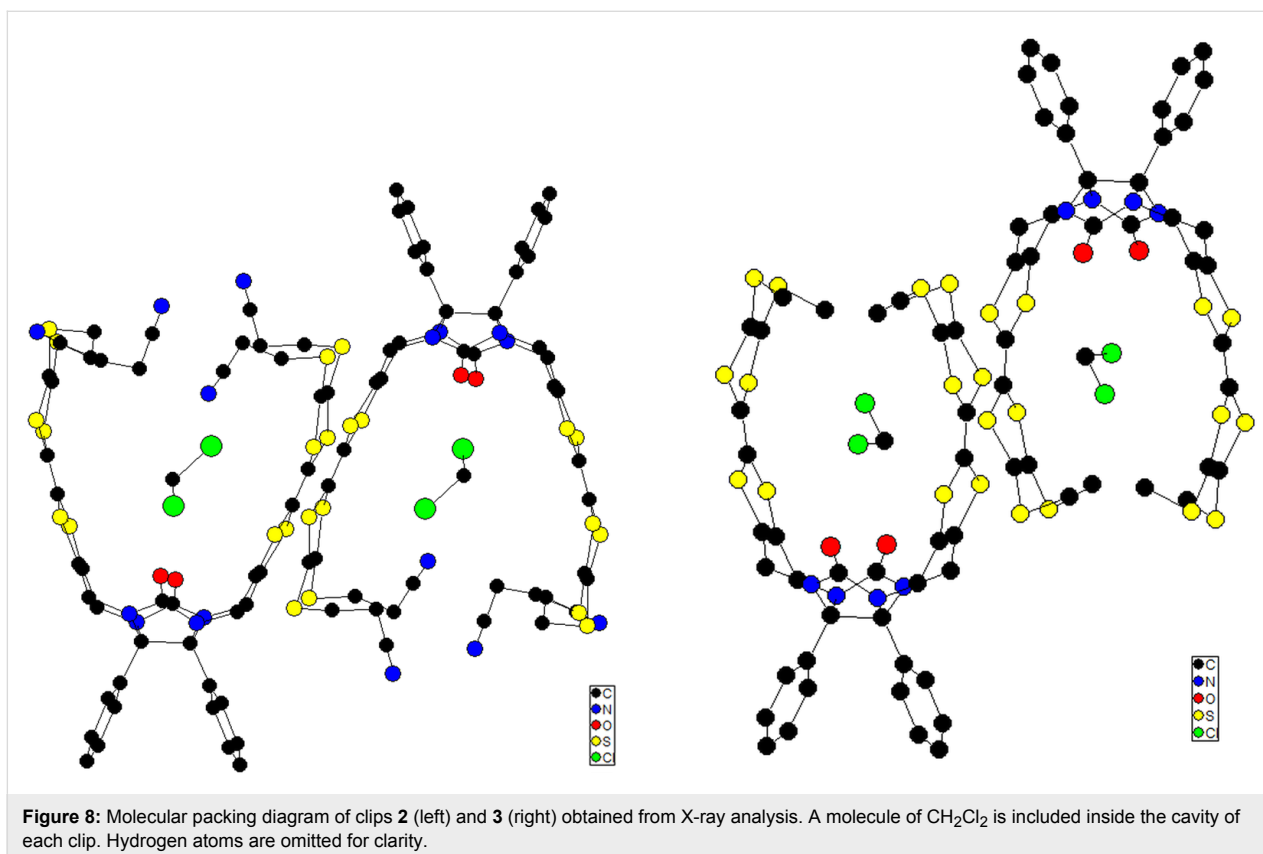


Figure 8: Molecular packing diagram of clips **2** (left) and **3** (right) obtained from X-ray analysis. A molecule of CH₂Cl₂ is included inside the cavity of each clip. Hydrogen atoms are omitted for clarity.

the basis of the size rather than the acceptor strength. We can suppose that the presence of stronger π -donor TTF sidewalls in clip **3** favorize donor–acceptor interactions and consequently the binding properties towards *m*-DNB. We have also checked the influence of the redox properties towards binding ability by studying the strong electrodeficient acceptor F₄-TCNQ.

Interaction with 1,3-dinitrobenzene (*m*-DNB)

The host–guest affinity was detected by UV–visible spectroscopy upon titration of clip **3** (10^{-3} M in *o*-C₆H₄Cl₂) with addition of *m*-DNB (10^{-1} M in *o*-C₆H₄Cl₂) aliquots. No additional change of the spectra was observed after the addition of one equivalent of *m*-DNB (-1.30 V vs Fc⁺/Fc) [65] which is in agreement with the formation of a 1:1 complex. A Job plot carried out in *o*-C₆H₄Cl₂ between clip **3** and *m*-DNB shows a maximum at 0.5, confirming the formation of the 1:1 complex (*m*-DNB@clip **3**) (Figure 9 left). The association constant was determined to be $K_a = (7 \pm 3) \times 10^3$ M⁻¹ by exploiting the Job plot analysis according to literature [66]. Despite many efforts devoted to the search for a complexation of *m*-DNB using molecular clip **4**, we could not observe any host–guest binding interaction. These results suggest that electronic and spatial properties of the cavity constitute fundamental parameters for binding the *m*-DNB guest. The binding of such a weak electron acceptor was successful for molecular clip **3** presenting the most suitable intramolecular distance between TTF sidewalls and the strongest π -donor ability.

Interaction with tetrafluoroquinodimethane (F₄-TCNQ)

The binding affinity of molecular clip **3** (5×10^{-4} M in CH₂Cl₂) was studied by a UV–visible titration with the electron acceptor

F₄-TCNQ (10^{-5} M in CH₂Cl₂). Addition of aliquots of molecular clip **3** onto a F₄-TCNQ solution showed the presence of an isosbestic point at 395 nm with the concomitant formation and increase of bands at 760 and 860 nm which could be attributed to the progressive formation of the F₄-TCNQ radical anion (Figure 10) [67,68]. The increase of the bands around 750 and 850 nm was attributed to the cumulative contribution of the increasing formation of TTF cation radical species and the F₄-TCNQ anion radical.

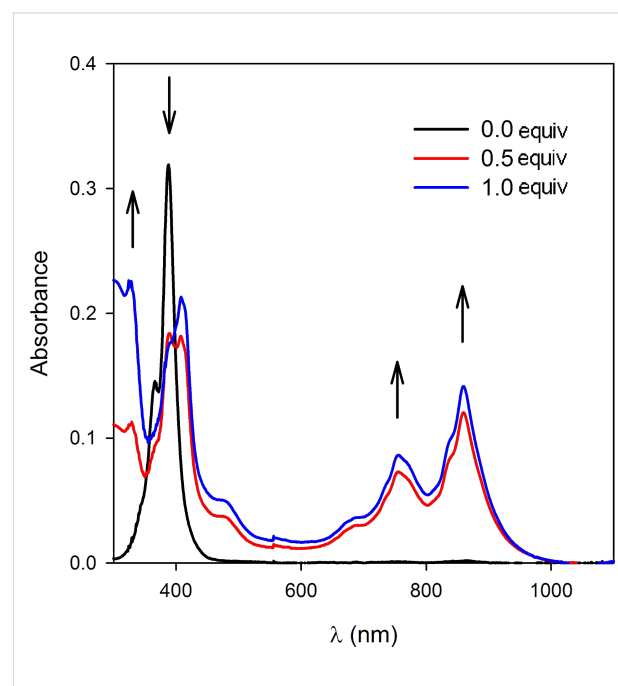


Figure 10: UV–visible absorption spectra of F₄-TCNQ (CH₂Cl₂, 10^{-5} M) upon titration with molecular clip **3** (CH₂Cl₂, 5×10^{-4} M).

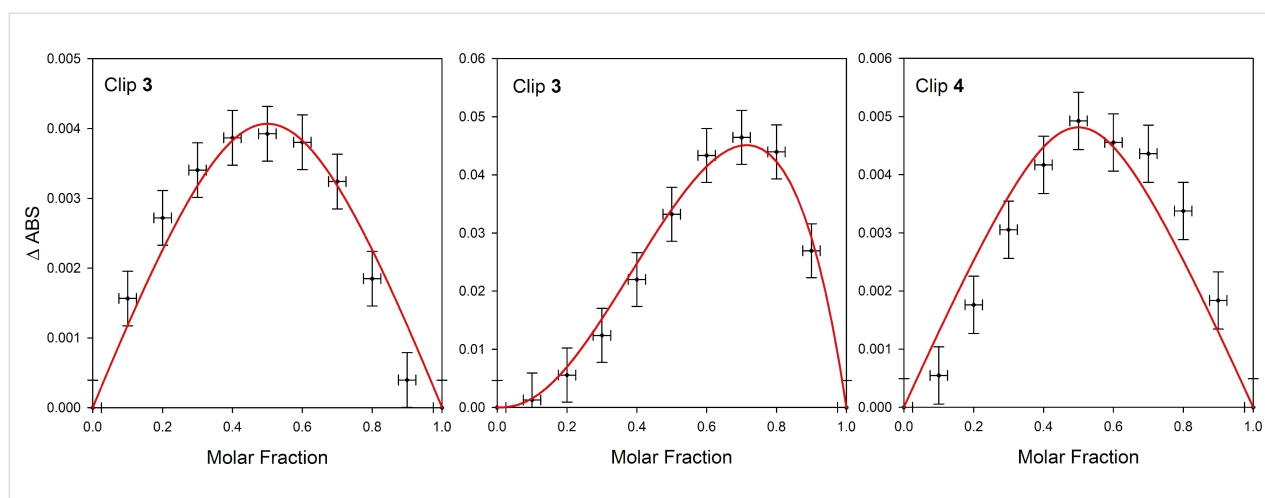


Figure 9: Left: Job plot analysis for DNB vs molecular clip **3** ($[3 + \text{DNB}] = 10^{-3}$ M in *o*-C₆H₄Cl₂ at 800 nm) at room temperature. Middle: Job plot for F₄-TCNQ vs molecular clip **3** at room temperature ($[3 + \text{F}_4\text{-TCNQ}] = 10^{-5}$ M in CH₂Cl₂ at 860 nm) consistent with a 2:1 binding stoichiometry. Right: Job plot for F₄-TCNQ vs molecular clip **4** at room temperature ($[4 + \text{F}_4\text{-TCNQ}] = 10^{-5}$ M in CH₂Cl₂ at 860 nm) in agreement with a 1:1 binding stoichiometry.

A Job plot carried out in CH_2Cl_2 between clip **3** and $\text{F}_4\text{-TCNQ}$ exhibited a maximum at around 0.7, a finding that corroborates with the formation of a 1:2 complex $(\text{F}_4\text{-TCNQ})_2@$ clip **3** (Figure 9 middle) with an average binding constant of $K_a = (8 \pm 5) \times 10^8 \text{ M}^{-1}$.

Similar studies were carried out using molecular clip **4** and quantitative measurements were performed using UV–visible titration considering the changes in the spectra of $\text{F}_4\text{-TCNQ}$ at 860 nm upon addition of sensor **4**. The construction of the Job plot is in agreement with the 1:1 binding stoichiometry between clip **4** and $\text{F}_4\text{-TCNQ}$ with a maximum centered at a molar ratio of 0.5 (Figure 9 right). The high association constant $K_a = (1.3 \pm 0.8) \times 10^6 \text{ M}^{-1}$ in CH_2Cl_2 confirms that this rigidified molecular clip **4** is an efficient receptor for $\text{F}_4\text{-TCNQ}$ guest electron acceptor.

This difference in binding interaction between host molecular clips **3** and **4** towards the $\text{F}_4\text{-TCNQ}$ guest could be explained by their electrochemical properties. By comparing the first oxidation potential of clips **3** and **4** with the first reduction potential of $\text{F}_4\text{-TCNQ}$ ($E_{\text{app}}^0_{\text{red1}} = +0.14 \text{ V vs Fc}^+/\text{Fc}$ – Figure 3), it is clear that $\text{F}_4\text{-TCNQ}$ guest presents a high reduction potential, sufficient to allow the oxidation of molecular clip **3**. Consequently, the $(\text{F}_4\text{-TCNQ})_2@$ clip **3** complex should result from a redox interaction between the host and the guest. On the other hand, the oxidation potential of molecular clip **4** is increased due to the introduction of the naphthoquinone spacer. Consequently, the corresponding 1:1 stoichiometry should reasonably

correspond to the binding of $\text{F}_4\text{-TCNQ}$ inside the cavity of clip **4** (Figure 11). This binding of $\text{F}_4\text{-TCNQ}$ also results from favourable spatial parameters with the increase of the intramolecular distance between the two TTF sidewalls. Thanks to the good π -donor ability of the TTF sidewalls, in combination with a well-suited size of the cavity, it is here demonstrated that molecular clip **4** constitutes one of the rare examples of systems exhibiting good affinity for sandwiching $\text{F}_4\text{-TCNQ}$ as an electron poor guest.

Conclusion

We have presented original synthetic strategies leading to glycoluril-based molecular clips containing electroactive TTF sidewalls. In particular, the one-step preparation of molecular clip using the N-tetraalkylation of glycoluril constitutes a powerful versatile method allowing an easy access to new architectures for which electrochemical properties can be tuned by simple modification of peripheral substituents on the TTF moiety. Cyclic voltammetry and spectroelectrochemical measurements demonstrated that the mixed-valence state in these fused glycoluril-TTF molecular clips seems to originate from intermolecular TTF interactions, according to measurements at various concentrations and to cyclic voltammogram simulations. Spatial and electrochemical properties were shown to be fundamental parameters towards the binding interaction of a weak (*m*-DNB) or strong ($\text{F}_4\text{-TCNQ}$) electrodeficient guest. Consequently, the selectivity for a given target guest could be precisely tuned via the choice of the molecular clip according to its electrochemical and spatial considerations.

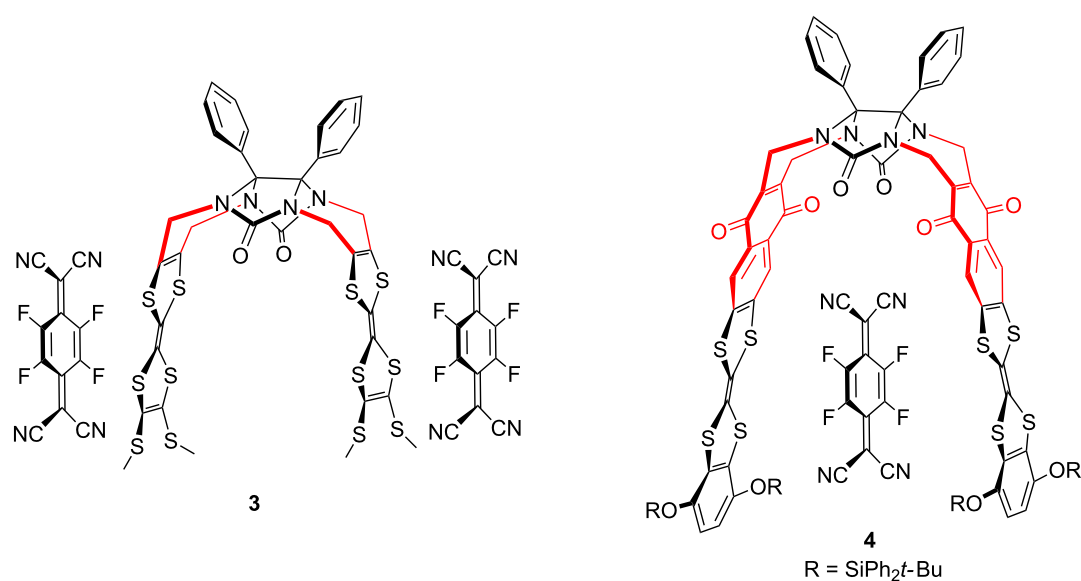


Figure 11: Redox interaction (left) and complexation (right) of $\text{F}_4\text{-TCNQ}$ with molecular clips **3** and **4**.

Experimental Synthesis

Molecular clips 1–3 [18] and 4 [19] were synthesized according to our previous reports.

Electrochemical and spectroelectrochemical experiments

Electrochemistry and time-resolved spectroelectrochemistry in solution were performed using the already described home self-made cell [44,45]. Electrochemical measurements were carried out using a platinum wire counter electrode and a silver wire as a quasi-reference electrode with a Biologic SP-150 potentiostat driven by the EC-Lab software including ohmic drop compensation. Experiments were recorded in dry HPLC-grade acetonitrile and dichloromethane with tetrabutylammonium hexafluorophosphate (Bu_4NPF_6 , electrochemical grade, Fluka) as supporting electrolyte. All solutions were prepared and transferred into the spectroelectrochemical cell in a glove box containing dry, oxygen-free (<1 ppm) argon, at room temperature.

Spectrophotometric measurements were carried out in direct reflexing mode on the working electrode (i.e., Pt or glassy carbon) with a homemade bench composed of different Princeton Instruments modules (light sources, fibers, monochromators, spectroscopy camera and software). The connection between the light source, the cell and the spectrophotometer is ensured through a “Y-shaped” optical fiber bundle: 18 fibers guide the light to the cell, and 19 fibers collect the reflected light from the cell to visible (320–1080 nm / maximum acquisition frequency 2 MHz) and IR (900–1700 nm / maximum acquisition frequency 8 MHz) CCD detectors. The sensitivity of the spectroscopic measurement (<3 electrons at 100 kHz and <13 electrons at 2 MHz between 320 and 1080 nm; 400 electrons (high gain) and 5000 electrons (low gain) between 900 nm and 1700 nm) allows performing a spectroelectrochemistry experiment under the usual conditions of electrochemistry.

Acknowledgements

This work was supported by the Ministère de la Recherche et de l'Enseignement Supérieur for Ph.D grants to Y. Cotelle and M. Hardouin-Lerouge.

References

- Wudl, F.; Smith, G. M.; Hufnagel, E. J. *J. Chem. Soc. D* **1970**, 1453–1454. doi:10.1039/C29700001453
- Bryce, M. R. *J. Mater. Chem.* **2000**, *10*, 589–598. doi:10.1039/A908385E
- Segura, J. L.; Martín, N. *Angew. Chem., Int. Ed.* **2001**, *40*, 1372–1409. doi:10.1002/1521-3773(20010417)40:8<1372::AID-ANIE1372>3.0.CO;2-I
- Yamada, J.; Sugimoto, T., Eds. *TTF Chemistry. Fundamentals and applications of tetrathiafulvalene*; Springer Verlag: New York, 2004.
- Gorgues, A.; Hudhomme, P.; Sallé, M. *Chem. Rev.* **2004**, *104*, 5151–5184. doi:10.1021/cr0306485
- Batail, P., Ed. Special issue on Molecular Conductors. *Chem. Rev.* **2004**, *104*, 4887–5782.
- Martín, N. *Chem. Commun.* **2013**, *49*, 7025–7027. doi:10.1039/C3CC00240C
- Bendikov, M.; Wudl, F.; Perepichka, D. F. *Chem. Rev.* **2004**, *104*, 4891–4946. doi:10.1021/cr030666m
- Bergkamp, J. J.; Decurtins, S.; Liu, S.-X. *Chem. Soc. Rev.* **2015**, *44*, 863–874. doi:10.1039/C4CS00255E
- Nielsen, M. O.; Lomholt, C.; Becher, J. *Chem. Soc. Rev.* **2000**, *29*, 153–164. doi:10.1039/A803992E
- Canevet, D.; Sallé, M.; Zhang, G.; Zhang, D.; Zhu, D. *Chem. Commun.* **2009**, 2245–2269. doi:10.1039/B818607N
- Steed, J. W.; Atwood, J. L. *Supramolecular Chemistry*, 2nd ed.; John Wiley & Sons Ltd, 2009.
- Hardouin-Lerouge, M.; Hudhomme, P.; Sallé, M. *Chem. Soc. Rev.* **2011**, *40*, 30–43. doi:10.1039/b915145c
- Chen, C.-W.; Whitlock, H. W., Jr. *J. Am. Chem. Soc.* **1978**, *100*, 4921–4922. doi:10.1021/ja00483a063
- Leblond, J.; Petitjean, A. *ChemPhysChem* **2011**, *12*, 1043–1051. doi:10.1002/cphc.201001050
- Sijbesma, R. P.; Nolte, R. J. M. *Top. Curr. Chem.* **1995**, *175*, 25–56. doi:10.1007/3-540-58800-0_17
- Rowan, A. E.; Elemans, J. A. A. W.; Nolte, R. J. M. *Acc. Chem. Res.* **1999**, *32*, 995–1006. doi:10.1021/ar9702684
- Cotelle, Y.; Allain, M.; Legoupy, S.; Hudhomme, P. *Org. Lett.* **2014**, *16*, 2590–2593. doi:10.1021/ol500458e
- Hardouin-Lerouge, M.; Cotelle, Y.; Legoupy, S.; Hudhomme, P. *New J. Chem.* **2014**, *38*, 5341–5348. doi:10.1039/c4nj00617h
- Butler, A. R.; Leitch, E. J. *Chem. Soc., Perkin Trans. 2* **1980**, 103–105. doi:10.1039/P29800000103
- Hudhomme, P.; Le Moustarder, S.; Durand, C.; Gallego-Planas, N.; Mercier, N.; Blanchard, P.; Levillain, E.; Allain, M.; Gorgues, A.; Riou, A. *Chem. – Eur. J.* **2001**, *7*, 5070–5083. doi:10.1002/1521-3765(20011203)7:23<5070::AID-CHEM5070>3.0.CO;2-6
- Reek, J. N. H.; Kros, A.; Nolte, R. J. M. *Chem. Commun.* **1996**, 245–247. doi:10.1039/CC9960000245
- Elemans, J. A. A. W.; Rowan, A. E.; Nolte, R. J. M. *J. Am. Chem. Soc.* **2002**, *124*, 1532–1540. doi:10.1021/ja012061i
- Creaven, B. S.; Gallagher, J. F.; McDonagh, J. P.; McGinley, J.; Murray, B. A.; Whelan, G. S. *Tetrahedron* **2004**, *60*, 137–143. doi:10.1016/j.tet.2003.10.084
- Wu, A.; Chakraborty, A.; Witt, D.; Lagona, J.; Damkaci, F.; Ofori, M. A.; Chiles, J. K.; Fettingner, J. C.; Isaacs, L. *J. Org. Chem.* **2002**, *67*, 5817–5830. doi:10.1021/jo0258958
- Wang, Z.-G.; Zhou, B.-H.; Chen, Y.-F.; Yin, G.-D.; Li, Y.-T.; Wu, A.-X.; Isaacs, L. *J. Org. Chem.* **2006**, *71*, 4502–4508. doi:10.1021/jo0603375
- Bogaschenko, T. Yu.; Lyapunov, A. Yu.; Kikot, L. S.; Mazepa, A. V.; Botoshansky, M. M.; Fonari, M. S.; Kirichenko, T. I. *Tetrahedron* **2012**, *68*, 4757–4764. doi:10.1016/j.tet.2012.04.009
- Easton, D. B. J.; Leaver, D. *Chem. Commun.* **1965**, 585–586. doi:10.1039/C19650000585
- Fabre, J.-M. *Chem. Rev.* **2004**, *104*, 5133–5150. doi:10.1021/cr0306440
- Svenstrup, N.; Rasmussen, K. M.; Hansen, T. K.; Becher, J. *Synthesis* **1994**, 809–812. doi:10.1055/s-1994-25580

31. Simonsen, K. B.; Becher, J. *Synlett* **1997**, 1211–1220. doi:10.1055/s-1997-1001
32. Hudhomme, P.; Liu, S.-G.; Kreher, D.; Cariou, M.; Gorgues, A. *Tetrahedron Lett.* **1999**, *40*, 2927–2930. doi:10.1016/S0040-4039(99)00325-1
33. Smeets, J. W. H.; Sijbesma, R. P.; Van Dalen, L.; Spek, A. L.; Smeets, W. J. J.; Nolte, R. J. M. *J. Org. Chem.* **1989**, *54*, 3710–3717. doi:10.1021/jo00276a037
34. Butler, A. R.; Hussain, I. *J. Chem. Soc., Perkin Trans. 2* **1981**, 310–316. doi:10.1039/P29810000310
35. Sijbesma, R. P.; Kentgens, A. P. M.; Lutz, E. T. G.; van der Maas, J. H.; Nolte, R. J. M. *J. Am. Chem. Soc.* **1993**, *115*, 8999–9005. doi:10.1021/ja00073a015
36. Baffreau, J.; Dumur, F.; Hudhomme, P. *Org. Lett.* **2006**, *8*, 1307–1310. doi:10.1021/ol060011i
37. Gautier, N.; Mercier, N.; Riou, A.; Gorgues, A.; Hudhomme, P. *Tetrahedron Lett.* **1999**, *40*, 5997–6000. doi:10.1016/S0040-4039(99)01162-4
38. Kreher, D.; Liu, S.-G.; Cariou, M.; Hudhomme, P.; Gorgues, A.; Mas, M.; Veciana, J.; Rovira, C. *Tetrahedron Lett.* **2001**, *42*, 3447–3450. doi:10.1016/S0040-4039(01)00494-4
39. Hudhomme, P. *C. R. Chim.* **2006**, *9*, 881–891. doi:10.1016/j.crci.2005.11.008
40. Bénard, C. P.; Geng, Z.; Heuft, M. A.; VanCrey, K.; Fallis, A. G. *J. Org. Chem.* **2007**, *72*, 7229–7236. doi:10.1021/jo0709807
41. Spanggaard, H.; Prehn, J.; Nielsen, M. B.; Levillain, E.; Allain, M.; Becher, J. *J. Am. Chem. Soc.* **2000**, *122*, 9486–9494. doi:10.1021/ja000537c
42. Azov, V. A.; Gómez, R.; Stelten, J. *Tetrahedron* **2008**, *64*, 1909–1917. doi:10.1016/j.tet.2007.11.110
43. Skibiński, M.; Gómez, R.; Lork, E.; Azov, V. A. *Tetrahedron* **2009**, *65*, 10348–10354. doi:10.1016/j.tet.2009.10.052
44. Gaillard, F.; Levillain, E. *J. Electroanal. Chem.* **1995**, *398*, 77–87. doi:10.1016/0022-0728(95)04144-1
45. Dias, M.; Hudhomme, P.; Levillain, E.; Perrin, L.; Sahin, Y.; Sauvage, F.-X.; Wartelle, C. *Electrochem. Commun.* **2004**, *6*, 325–330. doi:10.1016/j.elecom.2004.01.010
46. Alévêque, O.; Levillain, E.; Sanguinet, L. *Electrochem. Commun.* **2015**, *51*, 108–112. doi:10.1016/j.elecom.2014.12.014
47. Torrance, J. B.; Scott, B. A.; Welber, B.; Kaufman, F. B.; Seiden, P. E. *Phys. Rev. B* **1979**, *19*, 730–741. doi:10.1103/PhysRevB.19.730
48. Andreu, R.; Garín, J.; Orduna, J. *Tetrahedron* **2001**, *57*, 7883–7892. doi:10.1016/S0040-4020(01)00766-9
49. Khodorkovsky, V.; Shapiro, L.; Krief, P.; Shames, A.; Mabon, G.; Gorgues, A.; Giffard, M. *Chem. Commun.* **2001**, 2736–2737. doi:10.1039/B104934H
50. Rosokha, S. V.; Kochi, J. K. *J. Am. Chem. Soc.* **2007**, *129*, 828–838. doi:10.1021/ja064166x
51. Gautier, N.; Samuel, R.; Şahin, Y.; Levillain, E.; Leroy-Lhez, S.; Hudhomme, P. *Org. Lett.* **2004**, *6*, 1569–1572. doi:10.1021/ol049620l
52. Lyskawa, J.; Sallé, M.; Balandier, J.-Y.; Le Derf, F.; Levillain, E.; Allain, M.; Viel, P.; Palacin, S. *Chem. Commun.* **2006**, 2233–2235. doi:10.1039/B518275A
53. Coskun, A.; Spruell, J. M.; Barin, G.; Fahrenbach, A. C.; Forgan, R. S.; Colvin, M. T.; Carmieli, R.; Benítez, D.; Tkatchouk, E.; Friedman, D. C.; Sarjeant, A. A.; Wasielewski, M. R.; Goddard, W. A., III; Stoddart, J. F. *J. Am. Chem. Soc.* **2011**, *133*, 4538–4547. doi:10.1021/ja110584c
54. Ziganshina, A. Y.; Ko, Y. H.; Jeon, W. S.; Kim, K. *Chem. Commun.* **2004**, 806–807. doi:10.1039/B316651A
55. Yoshizawa, M.; Kumazawa, K.; Fujita, M. *J. Am. Chem. Soc.* **2005**, *127*, 13456–13457. doi:10.1021/ja053508g
56. Chen, P.-N.; Chiang, P.-T.; Chiu, S.-H. *Chem. Commun.* **2005**, 1285–1287. doi:10.1039/b417823h
57. Chiang, P.-T.; Cheng, P.-N.; Lin, C.-F.; Liu, Y.-H.; Lai, C.-C.; Peng, S.-M.; Chiu, S.-H. *Chem. – Eur. J.* **2006**, *12*, 865–876. doi:10.1002/chem.200500676
58. Chiang, P.-T.; Chen, N.-C.; Lai, C.-C.; Chiu, S.-H. *Chem. – Eur. J.* **2008**, *14*, 6546–6552. doi:10.1002/chem.200800213
59. Fumanal, M.; Capdevila-Cortada, M.; Miller, J. S.; Novoa, J. J. *J. Am. Chem. Soc.* **2013**, *135*, 13814–13826. doi:10.1021/ja405352p
60. Reek, J. N. H.; Elemans, J. A. A. W.; de Gelder, R.; Beurskens, P. T.; Rowan, A. E.; Nolte, R. J. M. *Tetrahedron* **2003**, *59*, 175–185. doi:10.1016/S0040-4020(02)01480-1
61. Chen, Y.; She, N.; Meng, X.; Yin, G.; Wu, A.; Isaacs, L. *Org. Lett.* **2007**, *9*, 1899–1902. doi:10.1021/ol0704340
62. Wu, A.; Chakraborty, A.; Fettingner, J. C.; Flowers, R. A.; Isaacs, L. *Angew. Chem., Int. Ed.* **2002**, *41*, 4028–4031. doi:10.1002/1521-3773(20021104)41:21<4028::AID-ANIE4028>3.0.CO;2-2
63. She, N.; Gao, M.; Cao, L.; Wu, A.; Isaacs, L. *Org. Lett.* **2009**, *11*, 2603–2606. doi:10.1021/ol900858d
64. Sijbesma, R. P.; Wijmenga, S. S.; Nolte, R. J. M. *J. Am. Chem. Soc.* **1992**, *114*, 9807–9813. doi:10.1021/ja00051a013
65. Macías-Ruvalcaba, N. A.; Evans, D. H. *J. Electroanal. Chem.* **2007**, *602*, 77–81. doi:10.1016/j.jelechem.2006.12.001
66. Renny, J. S.; Tomasevich, L. L.; Tallmadge, E. H.; Collum, D. B. *Angew. Chem., Int. Ed.* **2013**, *52*, 11998–12013. doi:10.1002/anie.201304157
67. Jain, A.; Rao, K. V.; Mogera, U.; Sagade, A. A.; George, S. J. *Chem. – Eur. J.* **2011**, *17*, 12355–12361. doi:10.1002/chem.201101813
68. Bivaud, S.; Balandier, J.-Y.; Chas, M.; Allain, M.; Goeb, S.; Sallé, M. *J. Am. Chem. Soc.* **2012**, *134*, 11968–11970. doi:10.1021/ja305451v

License and Terms

This is an Open Access article under the terms of the Creative Commons Attribution License (<http://creativecommons.org/licenses/by/2.0>), which permits unrestricted use, distribution, and reproduction in any medium, provided the original work is properly cited.

The license is subject to the *Beilstein Journal of Organic Chemistry* terms and conditions: (<http://www.beilstein-journals.org/bjoc>)

The definitive version of this article is the electronic one which can be found at: [doi:10.3762/bjoc.11.115](https://doi.org/10.3762/bjoc.11.115)